Supplementary Information Table 1. Information and spatial restraints for Integrative modeling of yeast and mouse basket. For each basket model (column 1), a list of experimental techniques is shown in column 2 that provides the spatial information (column 3) for Integrative modeling. Column 4 provides a reference to the original dataset or method.

Model	Experimental Technique	Spatial Information	Reference
Yeast	Quantitative mass spectrometry and biochemical quantification	Stoichiometry of Nups (SI Table 2)	(6)
	Chemical cross-linking with mass spectrometry readout	626 intra and intermolecular crosslinks among yNups and yMlps	(6, 24) & this study
	Cryo-ET	The overall shape of the basket including the basket distal density	this study
	Integrative models and atomic structural models	yNup84 complex dimer model yNup2 structural model (SI Table 2)	(5, 110, 111)
	Bioinformatics information	Sequence information coiled-coil propensities of the yMlps alignments. Connectivity between residues.	(109)
	Immuno-EM	Upper and lower bound on the N-/C- terminus of yMlps	(24)
	Biochemical experiments including *in vitro* binding assays proximity labeling	Interactions between yNup60^{MBM} (240-318) and yMlp1 (382-620) Interaction between yNup60^{N2BM} (505-539) and yNup2 (83-136) nuclear envelope binding domain of yNup1, yNup60	(26, 55)
Mouse/Human	Quantitative mass spectrometry and biochemical quantification	Stoichiometry of Nups (SI Table 3)	(112, 113)
	Cryo-ET	The overall shape of the basket including the basket distal density	this study
	Integrative models and atomic structural models	mNup107 complex dimer model mNup50 structural model (SI Table 3)	(35, 103, 104, 110, 111)
	Bioinformatics information	Sequence information coiled-coil propensities of the mTprs orthologs alignments. Connectivity between residues/beads. Structural equivalent distances between ortholog Nups.	(109)
	Immuno-EM	Upper and lower bound on the N-/C- terminus of mTprs	(102)
	Biochemical experiments including proximity labeling	Nuclear envelope binding domains of mNup153	(114)

Supplementary Information Table 2. Summary of the Integrative modeling of the yBaskets

(1) Gathering data	
Prior models	yNup84 complex dimer (PDB id: 7n84) (5) Position of yNup84 complex derived by fitting on cryo-ET map using the chimera fit map feature (96, 115). yNup2 alphaFold model (AF-P32499-F1-model-v4.pdb) (110, 111, 116).
Physical principles and statistical preferences	Excluded volume. Sequence connectivity
Experimental information	See SI Table 1
(2) Representing the system	
Sequences (Uniprot Ids)	yMlp1:Q02455, yMlp2:P40457, yMlp:Poly-ala of length yMlp1, yNup1:P20676, yNup2:P32499, yNup60:P39705, yNup120:P35729, yNup85:P46673, yNup145c:P49687, ySec13:Q04491, ySeh1:P53011, yNup84:P52891, yNup133:P36161
Composition (number of copies)	yMlp:2, yNup1:1, yNup2:2, yNup60:2, yNup120:2, yNup85:3, yNup145c:2, ySec13:2, ySeh1:2, yNup84:2, yNup133:2
Atomic (structured) components	yMlp.0: 71-183, 197-221, 239-281, 285-324, 340-371, 435-463, 535-570, 575-617, 622-668, 689-717, 745-773, 791-840, 844-893, 930-986, 990-1088, 1092-1127, 1143-1199, 1212-1251, 1254-1286, 1290-1339, 1343-1385, 1408-1457, yMlp.1: 71-183, 197-221, 239-281, 285-324, 340-371, 435-463, 535-570, 575-617, 622-668, 689-717, 745-773, 791-840, 844-893, 930-986, 990-1088, 1092-1127, 1143-1199, 1212-1251, 1254-1286, 1290-1339, 1343-1385, 1408-1457, yNup1.0: 1-32, 85-104, 106-123, yNup2.0: 83-136, 602-720, yNup2.1: 83-136, 602-720, yNup60.0: 27-47, 91-104, 106-119, 121-140, 142-162, yNup60.1: 27-47, 91-104, 106-119, 121-140, 142-162, yNup120.0: 1-29, 53-305, 311-711, 714-1036, yNup120.1: 1-29, 53-305, 311-711, 714-1036, yNup133.0: 63-183, 198-480, 490-763, 772-1155, yNup133.1: 56-77, 86-125, 133-144, 162-184, 193-200, 206-249, 258-480, 490-763, 772-1155, yNup145c.0: 119-712, yNup145c.1: 119-712, yNup84.0: 7-20, 27-80, 96-126, 136-364, 372-483, 506-562, 575-726, yNup84.1: 7-20, 27-80, 96-126, 136-364, 372-483, 506-562, 575-726, yNup85.0: 47-126, 132-230, 235-436, 451-744, yNup85.1: 47-126, 132-230, 235-436, 451-739, yNup85.2: 47-126, 132-230, 235-436, 451-739, ySec13.0: 8-157, 170-293, ySec13.1: 8-157, 170-293, ySeh1.0: 1-248, 288-346, ySeh1.1: 1-248, 288-346
Unstructured components	yMlp.0:-NTD: 1-70, yMlp.1:-NTD 1-70, yMlp.0:-LOOP: 184-196, 222-238, 282-284, 325-339, 372-434, 464-534, 571-574, 618-621, 669-688, 718-744, 774-790, 841-843, 894-929, 987-989, 1089-1091, 1128-1142, 1200-1211, 1252-1253, 1287-1289, 1340-1342, 1386-1407, yMlp.1:-LOOP: 184-196, 222-238, 282-284, 325-339, 372-434, 464-534, 571-574, 618-621, 669-688, 718-744, 774-790, 841-843, 894-929, 987-989, 1089-1091, 1128-1142, 1200-1211, 1252-1253, 1287-1289, 1340-1342, 1386-1407, yMlp.0:-CTD: 1458-1875, yMlp.1:-CTD: 1458-1875, yNup1.0: 33-84, 105-105, 124-335, yNup2.0: 51-82, yNup2.1: 51-82, yNup60.0: 1-26, 48-90, 105-105, 120-120, 141-141, 163-398, 505-539, yNup60.1: 1-26, 48-90, 105-105, 120-120, 141-141, 163-398, 505-539, yNup120.0: 30-52, 306-310, 712-713, 1037-103, yNup120.1: 30-52, 306-310, 712-713, 1037-1037, yNup133.0: 1-62, 184-197, 481-489, 764-771, 1156-1157, yNup133.1: 1-55, 78-85, 126-132, 145-161, 185-192, 201-205, 250-257, 481-489, 764-771, 1156-115, yNup145c.0: 1-118, yNup145c.1: 1-118, yNup84.0: 1-6, 21-26, 81-95, 127-135, 365-371, 484-505, 563-574, yNup84.1: 1-6, 21-26, 81-95, 127-135, 365-371, 484-505, 563-574, yNup85.0: 1-46, 127-131, 231-234, 437-450, yNup85.1: 1-46, 127-131, 231-234, 437-450, 740-744, yNup85.2: 1-46, 127-131, 231-234, 437-450, 740-744, ySec13.0: 1-7, 158-169, 294-297, ySec13.1: 1-7, 158-169, 294-297, ySeh1.0: 249-287, 347-349, ySeh1.1: 249-287, 347-349
Resolutions of structured omponents	1 [R1] residue per bead and 30 [R30] residue per bead
Resolutions of unstructured components	yMlp.0-NTD: 50 [R50] residue per bead, yMlp.1-NTD: 50 [R50] residue per bead, yMlp.0-LOOP: 5 [R5] residue per bead, yMlp.1-LOOP: 5 [R5] residue per bead, yMlp.0-CTD: 50 [R50] residue per bead, yMlp.1-CTD: 50 [R50] residue per bead, Rest all unstructured components 30 [R30] residue per bead
Structural coverage	77.39%
Spatial restraints encoded into scoring functions	Excluded volume; applied to the R30 representation. Sequence connectivity; applied to the R1 representation. Cross-link restraints; applied to the R1 representation.

Supplementary Information Table 2. Continued..

Rigid body (RB) definitions	RB1: yMlp.0 71-183, yMlp.1 71-183, RB2: yMlp.0 197-221, yMlp.1 197-221, RB3: yMlp.0 239-281, yMlp.1 239-281, RB4: yMlp.0 285-324, yMlp.1 285-324, RB5: yMlp.0 340-371, yMlp.1 340-371, RB6: yMlp.0 435-463,yMlp.1 435-463, RB7: yMlp.0 535-570, yMlp.1 535-570, RB8: yMlp.0 575-617, yMlp.1 575-617, RB9: yMlp.0 622-668, yMlp.1 622-668, RB10: yMlp.0 689-717, yMlp.1 689-717, RB11: yMlp.0 745-773, yMlp.1 745-773, RB12: yMlp.0 791-840, yMlp.1 791-840, RB13: yMlp.0 844-893, yMlp.1 844-893, RB14: yMlp.0 930-986, yMlp.1 930-986, RB15: yMlp.0 990-1088, yMlp.1 990-1088, RB16: yMlp.0 1092-1127, yMlp.1 1092-1127, RB17: yMlp.0 1143-1199, yMlp.1 1143-1199, RB18: yMlp.0 1212-1251, yMlp.1 1212-1251, RB19: yMlp.0 1254-1286, yMlp.1 1254-1286, RB20: yMlp.0 1290-1339, yMlp.1 1290-1339, RB21: yMlp.0 1343-1385, yMlp.1 1343-1385, RB22: yMlp.0 1408-1457, yMlp.1 1408-1457, RB23: yNup1.0 1-32, RB24: yNup1.0 85-104, RB25: yNup1.0 106-123, RB26: yNup2.0 83-136, RB27: yNup2.0 602-720, RB28: yNup2.1 83-136, RB29: yNup2.1 602-720, RB30: yNup60.0 27-47, RB31: yNup60.0 91-104, RB32: yNup60.0 106-119, RB33: yNup60.0 121-140, RB34: yNup60.0 142-162, RB35: yNup60.1 27-47, RB36: yNup60.1 91-104, RB37: yNup60.1 106-119, RB38: yNup60.1 121-140, RB39: yNup60.1 142-162, RB40: yNup120.0 1-29, yNup120.0 53-305, yNup120.0 311-711, yNup120.0 714-1036, RB41: yNup120.1 1-29, yNup120.1 53-305, yNup120.1 311-711, yNup120.1 714-1036, RB42: yNup85.0 47-126, yNup85.0 132-230, yNup85.0 235-436, yNup85.0 451-744, RB43: yNup85.1 47-126, yNup85.1 132-230, yNup85.1 235-436, yNup85.1 451-739, RB44: yNup85.2 47-126, yNup85.2 132-230, yNup85.2 235-436, yNup85.2 451-739, RB45: yNup145c.0 119-712, RB46: yNup145c.1 119-712, RB47: ySec13.0 8-157, ySec13.0 170-293, RB48: ySec13.1 8-157, ySec13.1 170-293, RB49: ySeh1.0 1-248, ySeh1.0 288-346, RB50: ySeh1.1 1-248, ySeh1.1 288-346, RB51: yNup84.0 7-20, yNup84.0 27-80, yNup84.0 96-126, yNup84.0 136-364, yNup84.0 372-483, yNup84.0 506-562, yNup84.0 575-726, RB52:yNup84.1 7-20, yNup84.1 27-80, yNup84.1 96-126, yNup84.1 136-364, yNup84.1 372-483, yNup84.1 506-562, yNup84.1 575-726, RB53: yNup133.0 63-183, yNup133.0 198-480, yNup133.0 490-763, yNup133.0 772-1155, RB54: yNup133.1 56-77, yNup133.1 86-125, yNup133.1 133-144, yNup133.1 162-184, yNup133.1 193-200, yNup133.1 206-249, yNup133.1 258-480, yNup133.1 490-763, yNup133.1 772-1155
(3) Structural sampling	
Sampling method	Replica Exchange Gibbs sampling, based on Metropolis Monte Carlo (105, 106)
Replica exchange temperature range	1.0 - 4.0
Number of replicas	4
Number of Independent runs	300
Number of structures generated	15,467,933
Movers for flexible string of beads	Random translation up to 10 Å
Total time for sampling	180 hours on 1200 processors
(4) Validating the yBasket models	
Models selected for validation	
Equilibrated models	2,335,171
Number of structures in samples A/B	All: 1,210,882 / 1,072,745
Number of structures selected for RMSD clustering sample A/B	Random sub-sample: 7,857 / 7,987
p-value of non-parametric Kolmogorov-Smirnov two-sample test	0.0556 (threshold p-value > 0.05)
Kolmogorov-Smirnov two-sample test statistic, D	0.0
Throughness of the structural sampling	
Sampling precision	70.41 Å
Homogeneity of proportions chi-squared-test (p-value)/Cramers V value	0.0/0.095 (thresholds: p-value<0.05 OR Cramer's V<0.1)
Number of clusters	5
Cluster populations	Cluster 1 : 93.5%, Cluster 2 : 4.0%, Cluster 3 : 1.2%, Cluster 4 : 1.0%, Cluster 5 : 0.3%
Cluster precisions	Cluster 1 : 57.2 Å, Cluster 2 : 58.6 Å, Cluster 3 : 56.5 Å, Cluster 4 : 53.3 Å, Cluster 5 : 59.8 Å
Average cross-correlation between localization probability densities of samples A and B	0.96
Validation by information used for modeling	
Percent of sequence connectivity restraints satisfied by ensemble	99%
Percent Excluded volume restraint satisfied by ensemble	Mean value 99.2% at R[30] resolution and mean value 99.9% at R[1] resolution
Cross-correlation between localization probability densities and cryo-ET map	0.82
Percent crosslink restraint satisfied by ensemble	94%
(5) Software and data availability	
Software	
Modeling programs	IMP PMI module, version-a41075a Integrative Modeling Platform (IMP), version 2.19 (https://integrativemodeling.org) (52). Gmconvert (117).
Modeling scripts	https://github.com/neeleshsoni21/Yeast_NPC_Basket
Structure prediction	AlphaFold2
Visualization and plotting	UCSF ChimeraX

Supplementary Information Table 3. Summary of the Integrative modeling of the mBaskets.

(1) Gathering data	
Prior models	mNup107 complex dimer comparative model built on Human Nup107 complex (PDB id: 7r5j) (35, 103, 104). Position of yNup107 complex derived by fitting on cryo-ET map using the chimera fit map feature (96, 115). yNup50 alphaFold model (AF-Q9JIH2-F1-model$_v4.pdb$) (110, 111, 116)
Physical principles and statistical preferences	Excluded volume. Sequence connectivity
Experimental information	See SI Table 1
(2) Representing the system	
Sequences (Uniprot Ids)	mTpr:F6ZDS4, mNup50:Q9JIH2, mNup153:E9Q3G8, mNup43:P59235, mSeh1:Q8R2U0, mNup98-mNup96:Q6PFD9, mNup85:Q8R480, mNup37:Q9CWU9, mNup107:Q8BH74, mSec13:Q9D1M0, mNup133:Q8R0G9, mNup160:Q9Z0W3
Composition (number of copies)	mTpr: 2, mNup50: 2, mNup153: 2, mNup107: 2, mNup133: 2, mNup160: 2, mNup37: 2, mNup43: 2, mNup85: 2, mNup96: 2, mSec13: 2, mSeh1: 2
Atomic (structured) components	mTpr.0: 96-120, 124-180, 187-247, 254-285, 289-356, 360-405, 413-451, 511-595, 639-681, 757-883, 901-946, 947-999, 1004-1060, 1064-1106, 1107-1131, 1135-1163 1170-1201, 1205-1254, 1281-1337, 1343-1420, 1424-1491, 1543-1616, 1627-1690, mTpr.1: 96-120, 124-180, 187-247, 254-285, 289-356, 360-405, 413-451, 511-595, 639-681, 757-883, 901-946, 947-999, 1004-1060, 1064-1106, 1107-1131, 1135-1163, 1170-1201, 1205-1254, 1281-1337, 1343-1420, 1424-1491, 1543-1616, 1627-1690, mNup50.0: 151-204, 355-466, mNup50.1: 151-204, 355-466, mNup153.0: 36-57, mNup153.1: 36-57, mNup107.0: 145-926, mNup107.1: 145-926, mNup133.0: 70-1155, mNup133.1: 70-1155, mNup160.0: 1-1402, mNup160.1: 1-1402, mNup37.0: 1-326, mNup37.1: 1-326, mNup43.0: 1-292, 327-380, mNup43.1: 1-292, 327-380, mNup85.0: 1-656, mNup85.1: 1-656, mNup96.0: 1111-1159, 1194-1816, mNup96.1: 1111-1159, 1194-1816, mSec13.0: 1-302, mSec13.1: 1-302, mSeh1.0: 1-324, mSeh1.1: 1-324
Unstructured components	mTpr.0:-NTD: 1-95, mTpr.1:-NTD: 1-95, mTpr.0:-LOOP: 121-123, 181-186, 248-253, 286-288, 357-359, 406-412, 452-510, 596-638, 682-756, 884-900, 1000-1003, 1061-1063, 1132-1134, 1164-1169, 1202-1204, 1255-1280, 1338-1342, 1421-1423, 1492-1542, 1617-1626, mTpr.1:-LOOP: 1-95, 121-123, 181-186, 248-253, 286-288, 357-359, 406-412, 452-510, 596-638, 682-756, 884-900, 1000-1003, 1061-1063, 1132-1134, 1164-1169, 1202-1204, 1255-1280, 1338-1342, 1421-1423, 1492-1542, 1617-1626, mTpr.0:-CTD: 1691-2431, mTpr.1:-CTD: 1691-2431, mNup50.0: 1-150, 205-354, mNup50.1: 1-150, 205-354, mNup153.0: 1-35, 58-428, 540-574, mNup153.1: 1-35, 58-428, 540-574
Resolutions of structured omponents	1 [R1] residue per bead and 30 [R30] residue per bead
Resolutions of unstructured components	mTpr.0-NTD: 50 [R50] residue per bead. mTpr.1-NTD: 50 [R50] residue per bead. mTpr.0-LOOP: 30 [R5] residue per bead. mTpr.1-LOOP: 30 [R5] residue per bead. mTpr.0-CTD: 50 [R50] residue per bead. mTpr.1-CTD: 50 [R50] residue per bead. Rest all unstructured components 30 [R30] residue per bead.
Structural coverage	79.48%
Rigid body (RB) definitions	RB1: mTpr.0 96-120, mTpr.1 96-120, RB2: mTpr.0 124-180, mTpr.1 124-180, RB3: mTpr.0 187-247, mTpr.1 187-247, RB4: mTpr.0 254-285, mTpr.1 254-285, RB5: mTpr.0 289-356, mTpr.1 289-356, RB6: mTpr.0 360-405, mTpr.1 360-405, RB7: mTpr.0 413-451, mTpr.1 413-451, RB8: mTpr.0 511-595, mTpr.1 511-595, RB9: mTpr.0 639-681, mTpr.1 639-681, RB10: mTpr.0 757-883, mTpr.1 757-883, RB11: mTpr.0 901-946, mTpr.1 901-946, RB12: mTpr.0 947-999, mTpr.1 947-999, RB13: mTpr.0 1004-1060, mTpr.1 1004-1060, RB14: mTpr.0 1064-1106, mTpr.1 1064-1106, RB15: mTpr.0 1107-1131, mTpr.1 1107-1131, RB16: mTpr.0 1135-1163, mTpr.1 1135-1163, RB17: mTpr.0 1170-1201, mTpr.1 1170-1201, RB18: mTpr.0 1205-1254, mTpr.1 1205-1254, RB19: mTpr.0 1281-1337, mTpr.1 1281-1337, RB20: mTpr.0 1343-1420, mTpr.1 1343-1420, RB21: mTpr.0 1424-1491, mTpr.1 1424-1491, RB22: mTpr.0 1543-1616, mTpr.1 1543-1616, RB23: mTpr.0 1627-1690, mTpr.1 1627-1690, RB24: mNup50.0 151-204, RB25: mNup50.0 355-466, RB26: mNup50.1 151-204, RB27: mNup50.1 355-466, RB28: mNup153.0 36-57, RB29: mNup153.1 36-57. Fixed RB components: RB30: mNup160.0 1-1402, RB31: mNup160.1 1-1402, RB32: mNup85.0 1-656, RB33: mNup85.1 1-656, RB34: mNup96.0 1111-1159, mNup96.0 1194-1816, RB35: mNup96.1 1111-1159, mNup96.1 1194-1816, RB36: mSec13.0 1-302, RB37: mSec13.1 1-302, RB38: mSeh1.0 1-324, RB39: mSeh1.1 1-324, RB40: mNup107.0 145-926, RB41: mNup107.1 145-926, RB42: mNup133.0 70-1155, RB43: mNup133.1 70-1155, RB44: mNup37.0 1-326, RB45: mNup37.1 1-326, RB46: mNup43.0 1-292, mNup43.0 327-380, RB47: mNup43.1 1-292, mNup43.1 327-380
Spatial restraints encoded into scoring functions	Excluded volume; applied to the R30 representation. Sequence connectivity; applied to the R1 representation. Cross-link restraints; applied to the R1 representation.

Supplementary Information Table 3. Continued..

(3) Structural sampling	
Sampling method	Replica Exchange Gibbs sampling, based on Metropolis Monte Carlo (105, 106)
Replica exchange temperature range	1.0 - 4.0
Number of replicas	2
Number of Independent runs	200
Number of structures generated	9,569,309
Movers for flexible string of beads	Random translation up to 10 Å
Total time for sampling	168 hours on 400 processors
(4) Validating the mBasket models	
Models selected for validation	
Equilibrated models	1,216,228
Number of structures in samples A/B	All: 520,767 / 474,386
Number of structures selected for RMSD clustering sample A/B	Random sub-sample: 6,886 / 7,783
p-value of non-parametric Kolmogorov-Smirnov two-sample test	0.056 (threshold p-value > 0.05)
Kolmogorov-Smirnov two-sample test statistic, D	0.0
Throughness of the structural sampling	
Sampling precision	52.9 Å
Homogeneity of proportions chi-squared-test (p-value)/Cramers V value	0.0/0.097 (thresholds: p-value<0.05 OR Cramer's V<0.1)
Number of clusters	4
Cluster populations	Cluster 1 : 75.6%, Cluster 2 : 15.6%, Cluster 3 : 8.1%, Cluster 4 : 0.7%
Cluster precisions	Cluster 1 : 41.9 Å, Cluster 2 : 34.9 Å, Cluster 3 : 41.2 Å, Cluster 4 : 31.4 Å
Average cross-correlation between localization probability densities of samples A and B	0.95
Validation by information used for modeling	
Percent of sequence connectivity restraints satisfied by ensemble	99%
Percent Excluded volume restraint satisfied by ensemble	Mean value 94.55% at R[30] resolution and mean value 99.63% at R[1] resolution
Cross-correlation between localization probability densities and cryo-ET map	0.87
(5) Software and data availability	
Software	
Modeling programs	IMP PMI module, version-a41075a Integrative Modeling Platform (IMP), version 2.19 (https://integrativemodeling.org) (52). Gmconvert (117).
Modeling scripts	https://github.com/neeleshsoni21/Mouse_NPC_Basket
Structure prediction	AlphaFold2
Visualization and plotting	UCSF ChimeraX

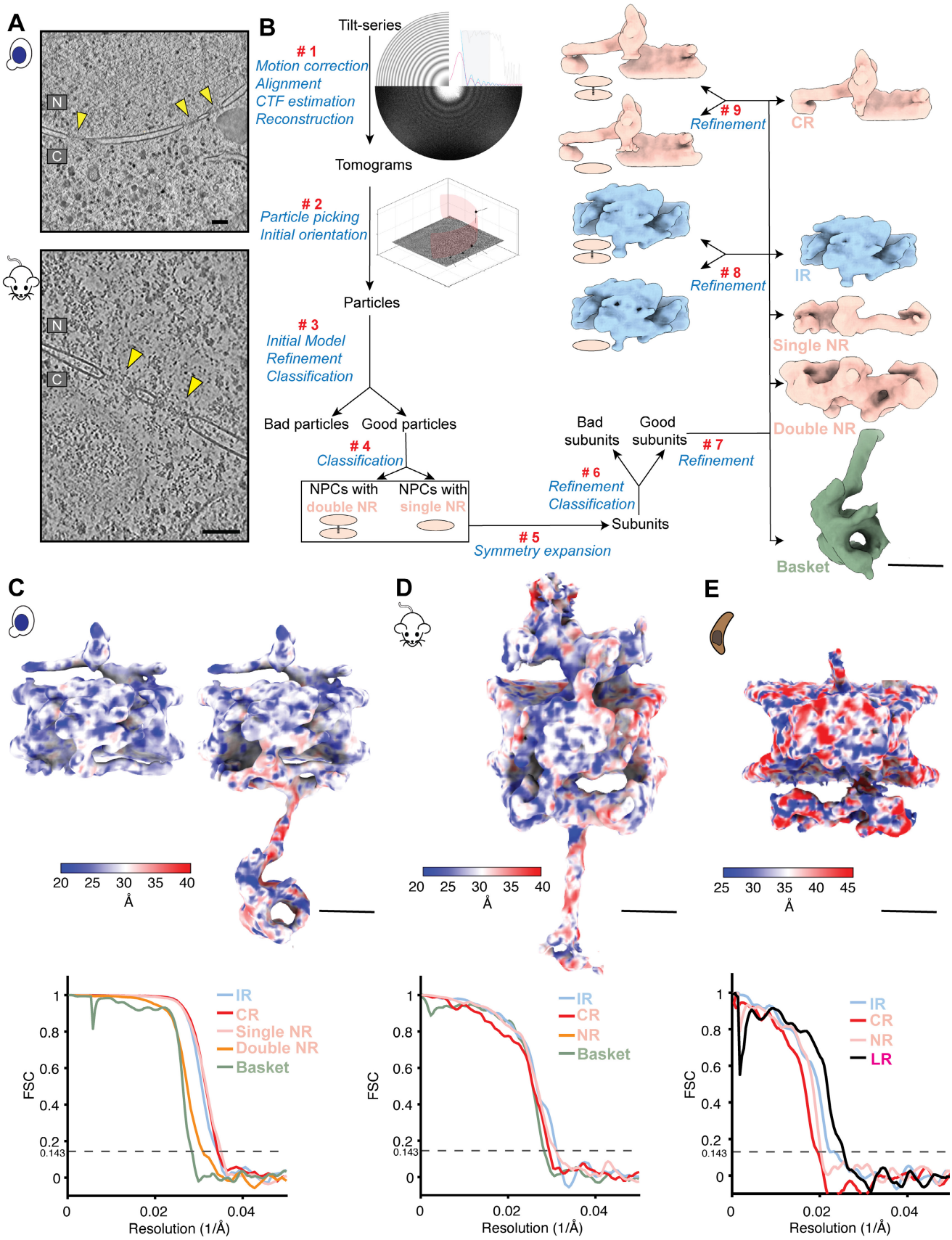

Fig. S1. Workflow of the subtomogram analysis of the NPC. (**A**) Slices of representative tomograms from yeast and mammalian cells, where nuclear pores are indicated by yellow arrows in the nucleus. Scale bar: 100 nm. (**B**) Processing workflow of the subtomogram analysis of the NPC, where steps are also indicated in red. The workflow is similar for data from all organisms. Some steps, like 4 for classifying out yNPCs with single and double NR, are more specific for yeast. For yeast, maps of the subunit of IR and CR from NPCs with single and double NR, as shown, resulting from steps 8 and 9 are similar. The same workflow was used for mNPC and pNPC. Scale bar: 200 Å. (C-E) Local resolution maps of the subunit of the NPC (top) along with Fourier shell correlation (FSC) curves of subunits of different rings (bottom) for yeast (**C**), mammalian (**D**), and *T. gondii.* (**E**). Scale bar: 200 Å. CR: Cytoplasmic ring, IR: Inner ring, NR: Nuclear ring, NE: Nuclear envelope, LR: Lumenal ring.

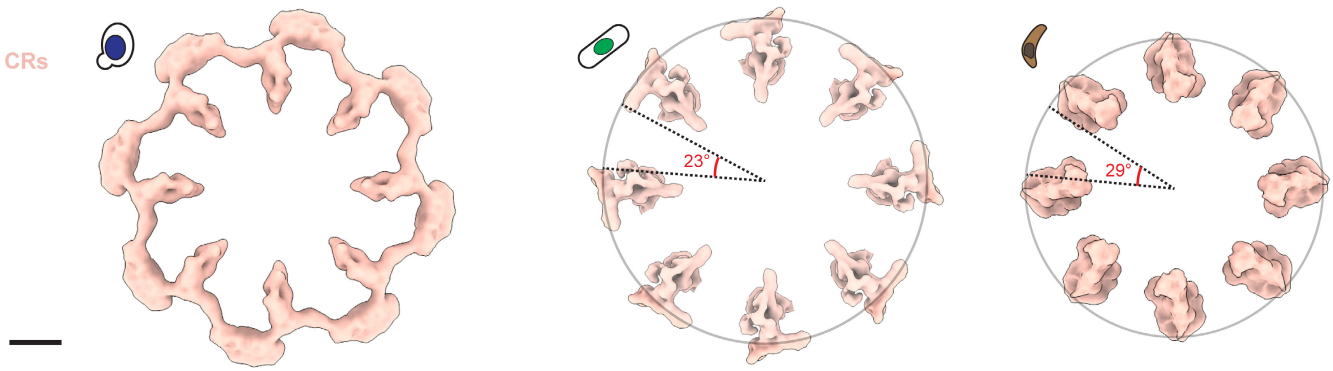

Fig. S2. CRs of NPCs from different organisms can have differing extents of completeness. (**A**) The circumference not covered (in central angles), by CRs of *S. cerevisiae* (left), *S. pombe* (middle; EMDB: 11373 (46) and *T. gondii* (right) is 0° (100-0%= 100% covered), 23° × 8 (100-51% = 49% covered), 29° × 8 (100-64% = 36% covered), respectively.

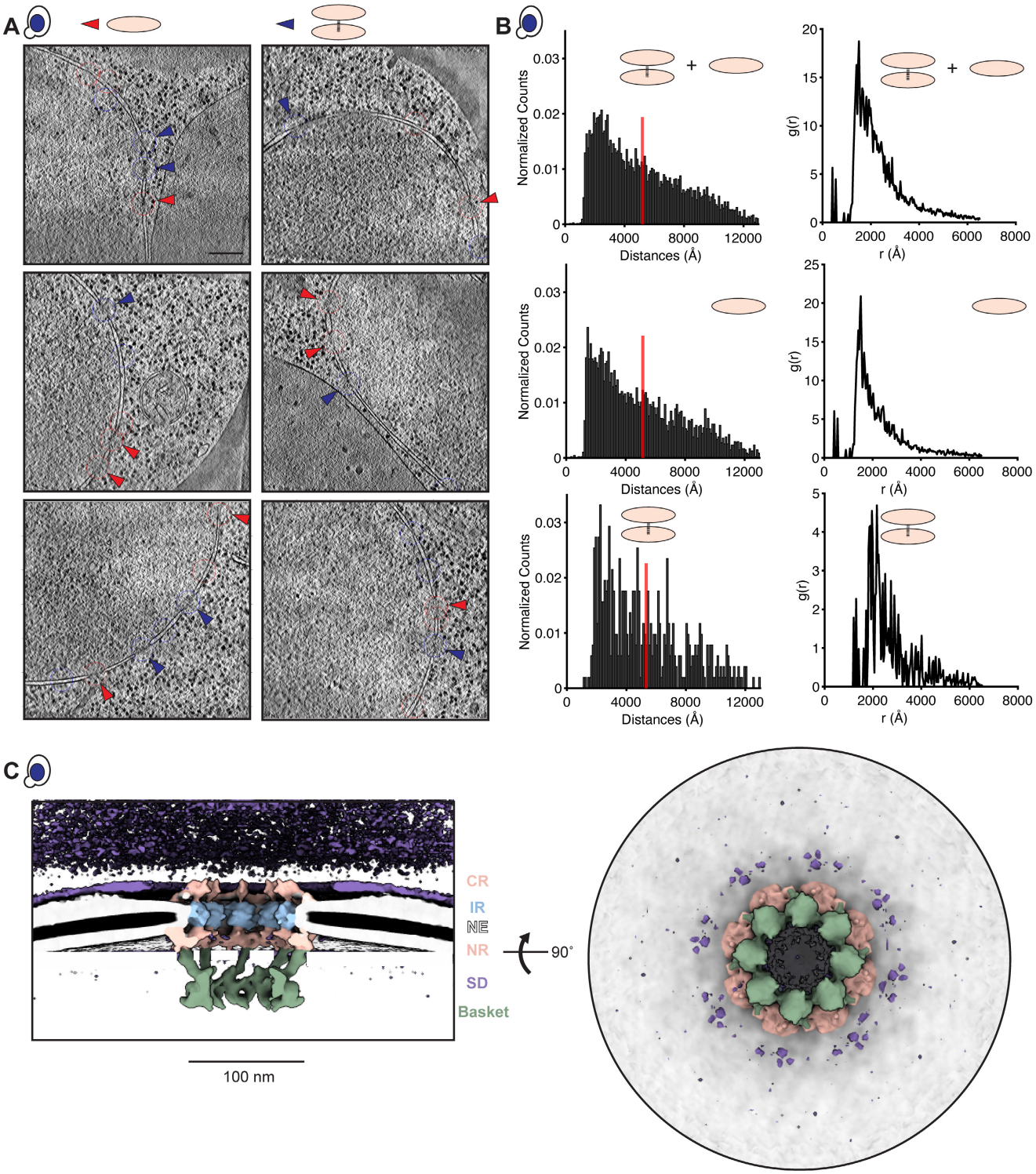

Fig. S3. yNPCs have less pronounced nuclear surrounding densities and their single and double NR variants are similarly distributed across the nucleus. (**A**) Slices of representative tomograms from yeast cells highlight yNPCs with single (indicated by red arrows) and double NRs (blue arrows). These images demonstrate that yNPCs with single and double NRs with a stable basket can be adjacent, rather than in distinctly separate areas. Scale bar: 100 nm. (**B**) Analysis of the yNPC's pairwise distance distribution (left) and the radial distribution function [g(r)] (right), encompassing all NPCs, as well as subsets with either single or double NRs, reveals a similar spatial distribution across the nucleus for all yNPCs. This is evidenced by the qualitative similarity in these distributions. (**C**) The cross-sectional (left) and nucleoplasmic view (right) of the map of yNPC shows the extent of crowding around the yNPC, with the surrounding densities (SD) shown at a very low isosurface threshold. These densities, compared to their counterpart in mNPCs, are much weaker.

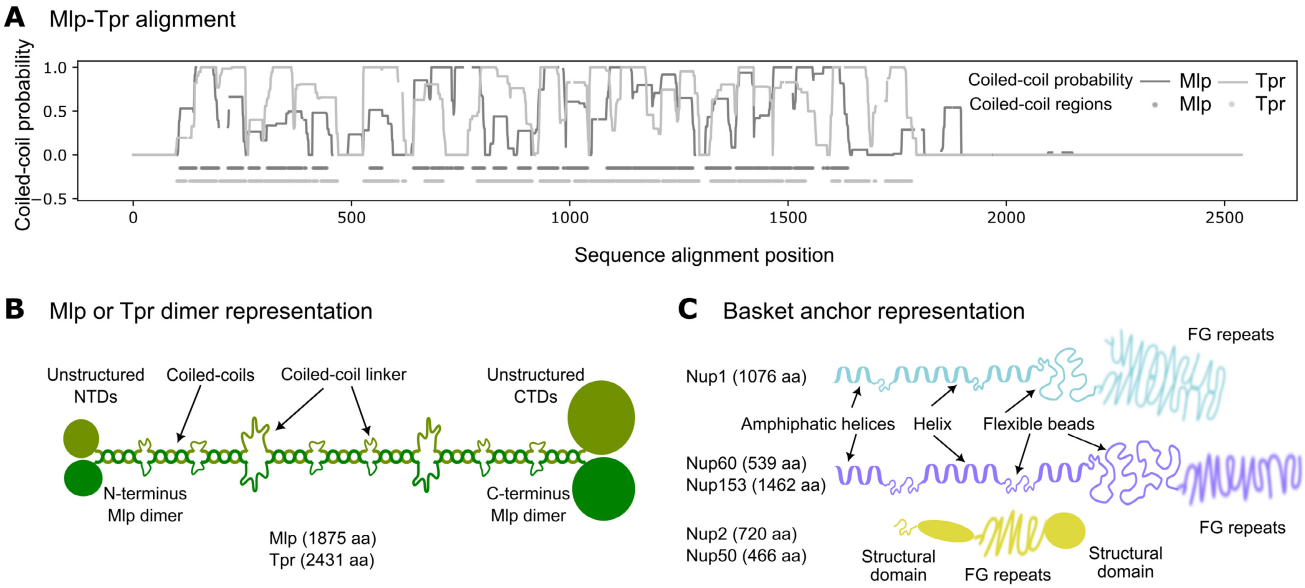

Fig. S4. Nuclear basket model representation. (**A**) Coiled-coil probabilities of yMlp (dark gray) and mTpr (light gray) at different positions in their sequence. The region represented as coiled-coil segments is shown as horizontal dots in a straight line below 0.0. (**B**) Schematic representation of a yMlp or mTpr dimer. Coiled-coil regions were represented as rigid bodies and linked through flexible strings of beads. The unstructured N- and C- terminal regions were represented as flexible strings of beads. (**C**) Schematic representation of the FG NR anchor Nups: yNup1, yNup2/mNup50, yNup60/mNup153. All structural regions, including amphipathic helices (AH) at the N terminus, were represented as rigid helices; all non-structural regions, excluding FG repeats, were represented as flexible strings of beads. FG repeats were not included in the model. The number of amino acid (aa) residues for different Nups are indicated in parenthesis.

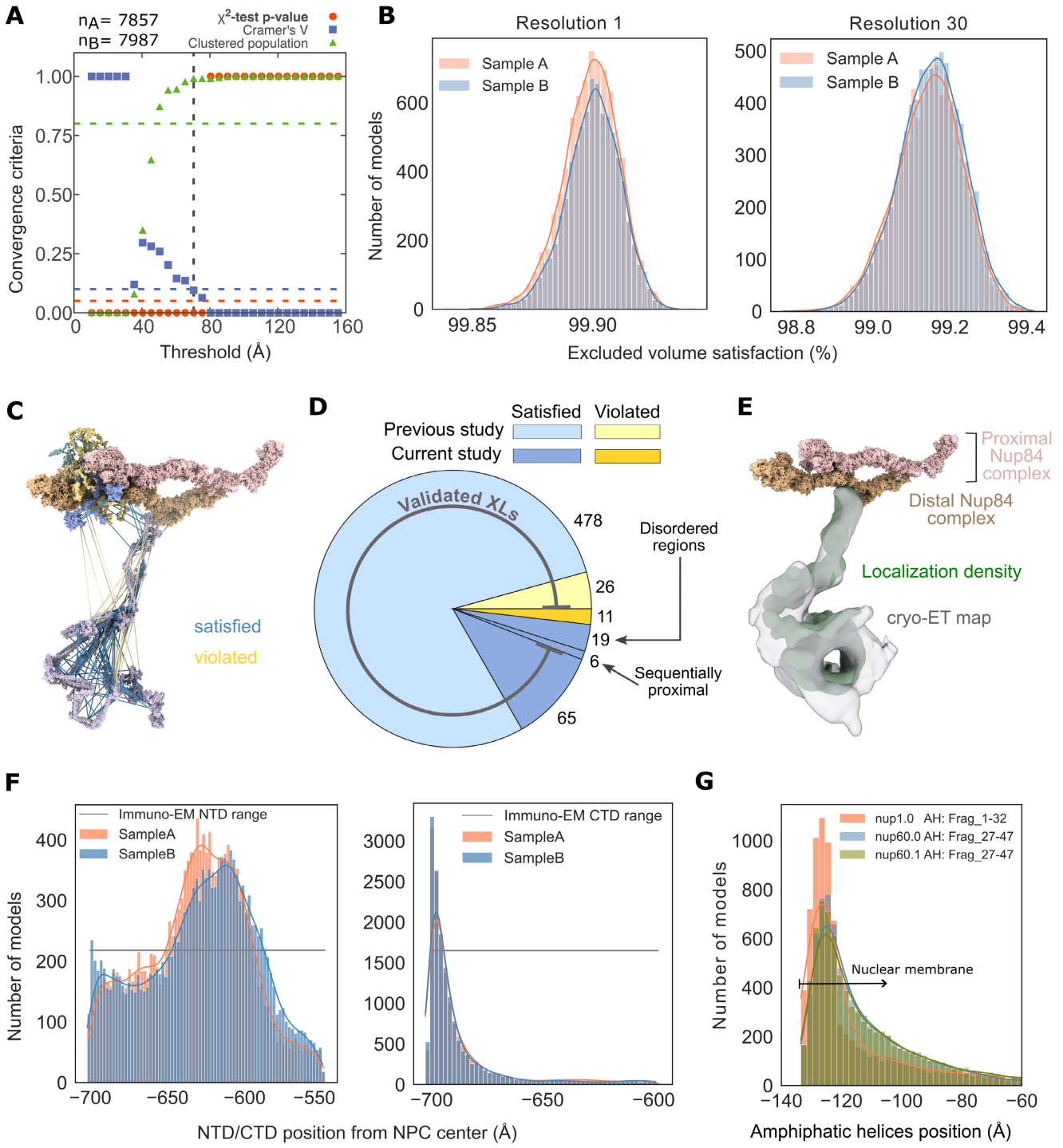

Fig. S5. Validation of integrative models of the yBasket. (**A**) Criteria for determining the sampling precision (y-axis), were evaluated as a function of the RMSD clustering threshold (x-axis) (n=15,844 models). First, the P value is computed using the chi-squared-test (one-sided) for homogeneity of proportions (red dots). Second, an effect size for the chi-squared-test is quantified by the Cramers's V value (blue squares). Third, the population of the structures in sufficiently large clusters is shown as green triangles. The vertical dotted grey line indicates the RMSD clustering threshold at which three conditions are satisfied (Cramer's V (0.095)<0.1 (blue horizontal dotted lines), P value (0.0)<0.05 and the population of clustered structures (0.99)>0.8 (green horizontal dotted lines, thus defining the sampling precision of 70.4 Å. The three solid curves (red, blue, and green) were drawn through the points to help visualize the results. The number of models in two randomly drawn samples, sample A and sample B, from a pool of filtered models (n=2,283,627 models) is denoted by nA (7857 models) and nB (7987 models). (**B**) Histogram of excluded volume restraint satisfaction of samples nA and nB at two different resolutions of 1 and 30 residues per bead. (**C**) Chemical cross-links were mapped onto the structure of the yBasket subunit with lines. Satisfied crosslinks where Euclidian Ca–Ca distances below 35 Å in the model ensemble are represented with blue lines, whereas violated crosslinks are with red lines. (**D**) A pie chart of satisfied (shades of blue) and violated (shades of yellow) crosslinks grouped into previously published (6) (light blue and light yellow) and current study (dark blue and dark yellow) crosslinks. The validated crosslinks (gray arc) account for 94% of the crosslinks; validated crosslinks have MS2 spectra with multiple backbone fragmentations of both peptides and peptides of at least 6 residues. Of the non-validated crosslinks, 11 were violated, 6 were trivially satisfied due to sequence proximity, and 19 were in the disordered/N-terminus/C-terminus regions of the basket distal density of our model. (**E**) A side view of the yBasket models localization density attached to the distal yNup84 complex spans most of the cryo-ET density map. (**F**) Satisfaction of experimentally derived range (gray line) of the position of yMlps N- and C-terminus by the model ensemble derived values (coral and light blue). (**G**) Satisfaction of experimentally derived range (gray line) of the position of amphipathic transmembrane helices of yNup1 and yNup60 by the model ensemble derived values (coral and light blue).

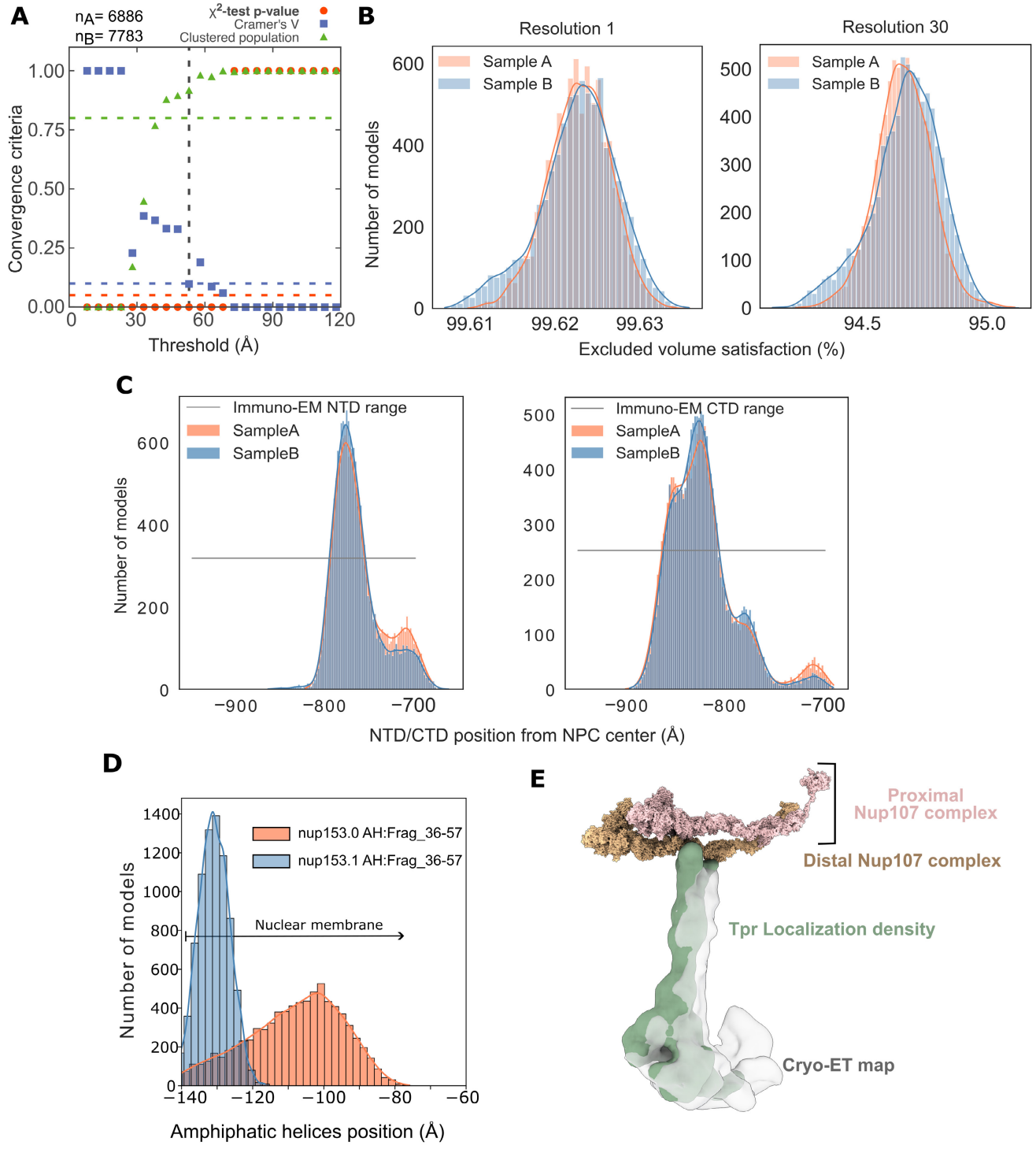

Fig. S6. Validation of integrative models of the mBasket. (**A**) Criteria for determining the sampling precision (y-axis), were evaluated as a function of the RMSD clustering threshold (x-axis) (n=14,669 models). First, the P value is computed using the chi-squared-test (one-sided) for homogeneity of proportions (red dots). Second, an effect size for the chi-squared-test is quantified by the Cramers's V value (blue squares). Third, the population of the structures in sufficiently large clusters is shown as green triangles. The vertical dotted grey line indicates the RMSD clustering threshold at which three conditions are satisfied (Cramer's V (0.097)<0.1 (blue horizontal dotted lines), P value (0.0)<0.05 and the population of clustered structures (0.92)>0.8 (green horizontal dotted lines, thus defining the sampling precision of 52.9 Å. The three solid curves (red, blue, and green) were drawn through the points to help visualize the results. The number of models in two randomly drawn samples from a pool of filtered models (n=995,151 models) is denoted by nA (6886 models) and nB (7783 models). (**B**) Histogram of excluded volume restraint satisfaction of samples nA and nB at two different resolutions of 1 and 30 residues per bead. (**C**) Satisfaction of experimentally derived range (gray line) of the position of mTpr's N- and C-terminus by the model ensemble derived values (coral and light blue). (**D**) Satisfaction of the experimentally derived range (gray line) of the position of amphipathic transmembrane helices of mNup153 by the model ensemble derived values (coral and light blue). (**E**) A side view of the mBasket models localization density attached to the distal mNup107 complex spans most of the cryo-ET density map.